Article

Thermoplastic Polymer Nanocomposites Based on Inorganic Fullerene-like Nanoparticles and Inorganic Nanotubes

Mohammed Naffakh [1],* and Ana M. Díez-Pascual [2]

[1] Departamento de Ingeniería y Ciencia de los Materiales, Escuela Técnica Superior de Ingenieros Industriales, Universidad Politécnica de Madrid, José Gutiérrez Abascal 2, 28006 Madrid, Spain

[2] Instituto de Ciencia y Tecnología de Polímeros (ICTP-CSIC), Juan de la Cierva 3, 28006 Madrid, Spain; E-Mail: adiez@ictp.csic.es

* Author to whom correspondence should be addressed; E-Mail: mohammed.naffakh@upm.es; Tel.: +34-913-363-164; Fax: +34- 913-363-007.

Abstract: Using inorganic fullerene-like (IF) nanoparticles and inorganic nanotubes (INT) in organic-inorganic hybrid composite, materials provide the potential for improving thermal, mechanical, and tribological properties of conventional composites. The processing of such high-performance hybrid thermoplastic polymer nanocomposites is achieved via melt-blending without the aid of any modifier or compatibilizing agent. The incorporation of small quantities (0.1–4 wt.%) of IF/INTs (tungsten disulfide, IF-WS$_2$ or molybdenum disulfide, MoS$_2$) generates notable performance enhancements through reinforcement effects and excellent lubricating ability in comparison with promising carbon nanotubes or other inorganic nanoscale fillers. It was shown that these IF/INT nanocomposites can provide an effective balance between performance, cost effectiveness, and processability, which is of significant importance for extending the practical applications of diverse hierarchical thermoplastic-based composites.

1. Introduction

Over the past few years, research interest in the field of thermoplastic composites has changed from "high-performance" advanced materials towards the development of "cost-performance" engineering composites. Especially, carbon fiber (CF) or glass fiber (GF) reinforced, thermoplastic-based composites have shown to offer design, processing, performance, and cost advantages compared to metals for manufacturing structural parts. Among the advantages provided by fiber-reinforced thermoplastics over metals and ceramics, that have been recognized for years, are improved fracture toughness, impact resistance, strength to weight ratio, as well as high resistance to corrosion and enhanced thermal and fatigue properties that have often been put in good use for practical applications in the aeronautic, automotive, and energy sectors [1–3]. Nevertheless, these applications require new properties and functionalities, especially superior mechanical performance, flame and chemical resistance, magnetic field and UV resistance, high electrical conductivity, environmental stability, low water absorption, and so forth. To address these issues, the integration of inorganic nanoparticles into a polymer matrix allows both properties from inorganic nanoparticles and polymer to be combined, thus, resulting in advanced polymer nanocomposites (PNCs) [4]. In particular, additional nanoscale fillers, such as carbon nanotubes (CNTs) [5] or inorganic nanoparticles [6], have been mixed with CFs to reinforce polymer matrices. Their high specific surface area enables the formation of a large interphase in the composite and strong filler-matrix interactions. In the same way, the addition of nanoclays to fiber-reinforced thermoplastic composites has been reported to improve damping properties, fatigue life, toughness, and wear resistance [7,8]. The synergetic effect of CFs with the inorganic nanoparticles is believed to be the major cause for the mechanical improvement achieved.

Recently, inorganic fullerenes (IFs) and nanotubes (INTs), based on layered metal dichalcogenides, such as WS_2 and MoS_2, have emerged as one of the most promising developments in the area of nanomaterials. These types of nanoparticles are currently the subject of intense research, summarized in these reviews that include synthetic methodologies, diverse properties of these new nanomaterials and their potential applications [9,10]. The first synthesis of such nanoparticles was reported by Tenne *et al.*, in 1992 and 1993 [11,12]. Since then, the synthetic technology has advanced considerably and almost pure materials (>99%) are currently synthesized in large amounts by ApNano Materials, Inc. (NanoMaterials, Ltd., Yavne, Israel) and employed in a wide variety of fields, such as aerospace, automotive, naval, defense, medical, energy, electronics, and various other industries. The physical properties of WS_2 and MoS_2 nanostructures (IF/INTs) have been studied in detail, both experimentally and by theoretical modeling. These properties are interesting, not only academically, but also because these kinds of nanostructures show substantial potential for becoming part of the ultrahigh-strength nanocomposite technology [13].

The objective of this article is to emphasize the most recent findings about the influence of IF nanoparticles and INTs on the structure, morphology and properties of thermoplastic polymer nanocomposites, in comparison with PNCs incorporating other nanofillers. Particular interest has been devoted to analyze the thermal, mechanical, and triblolological property enhancements attained in multiscale fiber-reinforced thermoplastic composites containing inorganic fullerene-like WS_2 nanoparticles.

2. Preparation and Dispersion of IF/INT into Thermoplastic Polymers

The mixing of polymers and nanoparticles is opening new avenues of research and development of advanced engineering flexible composites that exhibit advantageous magnetic, electrical, optical, or mechanical properties. The main challenge in fabrication of these polymer nanocomposites for structural and functional applications is uniform dispersion of nanoparticles in the polymer matrix. However, good dispersion of nanoparticles in polymer composite materials is extremely difficult to achieve since nanoparticles have a strong tendency to aggregate due to their nano-size and high surface energy. In the case of organic–inorganic nanocomposites, the strength or level of interaction between the organic and inorganic phases is another important factor in improving the overall properties of the composites. Physical or simple mechanical mixing usually lead to a weak interaction between the phases via hydrogen bonding or van der Waals forces. In order to minimize interface energies between particles and polymer matrices, several surface modification/functionalization and stabilization techniques have been developed that are mainly used in chemical methods, such as sol-gel, *in situ* polymerization, *etc*. Owing to numerous papers published on polymer organic–inorganic composite materials, it is impossible to completely review this field. The reader is referred to the literature cited for a more detailed description of synthetic methods used for the processing of PNCs reinforced with different types of inorganic nanofillers [13–15].

Inorganic layered materials, such as transition metal dichalcogenides MS_2 (M = Mo, W), are one of the most modern and the most promising development areas in the field of nanomaterials. Inorganic fullerene-like (IF) nanoparticles can provide significant advantages over other spherical nanoparticles for the preparation of advanced PNCs [13]. In particular, the incorporation of environmentally-friendly IF-WS_2 nanoparticles has been shown to improve thermal, mechanical, and tribological properties of a series of thermoplastic polymers, including isotactic polypropylene (iPP) [16], polyphenylene sulfide (PPS) [17], poly(ether ether ketone) (PEEK) [18], and nylon-6 [19]. The efficient dispersion of IF-WS_2 was achieved through simple melt-blending without using modifiers or surfactants. Moreover, the combination of inorganic fullerenes with other organic micro-particles (nucleating agents), micro-fibers (CFs) or nanofillers (CNTs) allows tailoring of more sophisticated hybrid materials with complex architectures, interactions, morphology, and functionality [20–24]. In the same way, the use of INT-WS_2 (MoS_2) offers the opportunity to produce novel advanced polymer nanocomposite materials with excellent nanoparticle dispersion. More specifically, since the beginning of 2011, we have successfully developed a new family of nanocomposites, which integrated MoS_2 nanotubes into an isotactic polypropylene (iPP) matrix, one of the most widely investigated polymers in the preparation and application of nanocomposites, employing a simple and cost effective melt-processing route [25]. This strategy yields finer dispersion, with INT-MoS_2 almost fully debundled into individual tubes or small clusters, which are randomly oriented in the iPP matrix. Additionally, well-dispersed WS_2 inorganic nanotubes were efficiently incorporated into epoxy matrix, poly(methyl methacrylate) (PMMA), poly(propylene fumarate) (PPF), and poly(3-hydroxybutyrate) (PHB), using various processing techniques [26–29]. Figure 1 shows, as an example, typical SEM images of the fracture surfaces of composites containing inorganic fullerene-like nanoparticles or inorganic nanotubes obtained under optimal processing conditions. It has been demonstrated by statistical analysis of the surface density of IF-WS_2 nanoparticles in the iPP nanocomposites, that the degree of dispersion strongly depends on the

duration of melt blending [16]. For 1.0 wt.% IF-WS$_2$ (Figure 1a), it can be seen that these nanoparticles are almost spherical, with an average diameter of around 80 nm, similar to that observed for the raw nanofiller, and are individually dispersed for mixing times between 5 and 20 min. However, for IF-WS$_2$ contents $\geq$ 4.0 wt.%, 5 min is not enough time to attain single particle distribution, and for the highest concentration incorporated of 8.0 wt.% (not shown here), the influence of the mixing time on the degree of dispersion is even stronger. With increasing loading, the interparticle distance decreases, hence, flocculation of these nanoparticles can occur after the mixing is stopped. Thus, the crystallization rate, as well as the modulus of iPP, initially rise with increasing filler content and finally level-off at filler loadings of around 1.0 wt.% [16]. In the case of multiscale fiber-reinforced thermoplastic composites, the laminates were prepared by the film-stacking process. Four layers of GF or CF were alternatively stacked within five iPP/IF-WS$_2$ (PPS/IF-WS$_2$) films in a closed mold. Consolidation of the material was made at 210 °C in a hot-press (320 °C in the case of PPS matrix) [22,23]. The results obtained are very promising and suggest that the use of IF/INT can provide an effective balance between cost effectiveness and processability, making the resulting polymer nanocomposites highly suitable for a wide range of applications at a large scale.

**Figure 1.** SEM micrographs of novel polymer/IF(INT) nanocomposites. (**a**) iPP/IF-WS$_2$ (1.0 wt.%); (**b**) PPS/IF-WS$_2$ (1.0 wt.%); (**c**) iPP/INT-MoS$_2$ (1.0 wt.%); (**d**) iPP/IF-WS$_2$ (2.0 wt.%)/GF and (**e**) PPS/IF-WS$_2$ (2.0 wt.%)/CF.
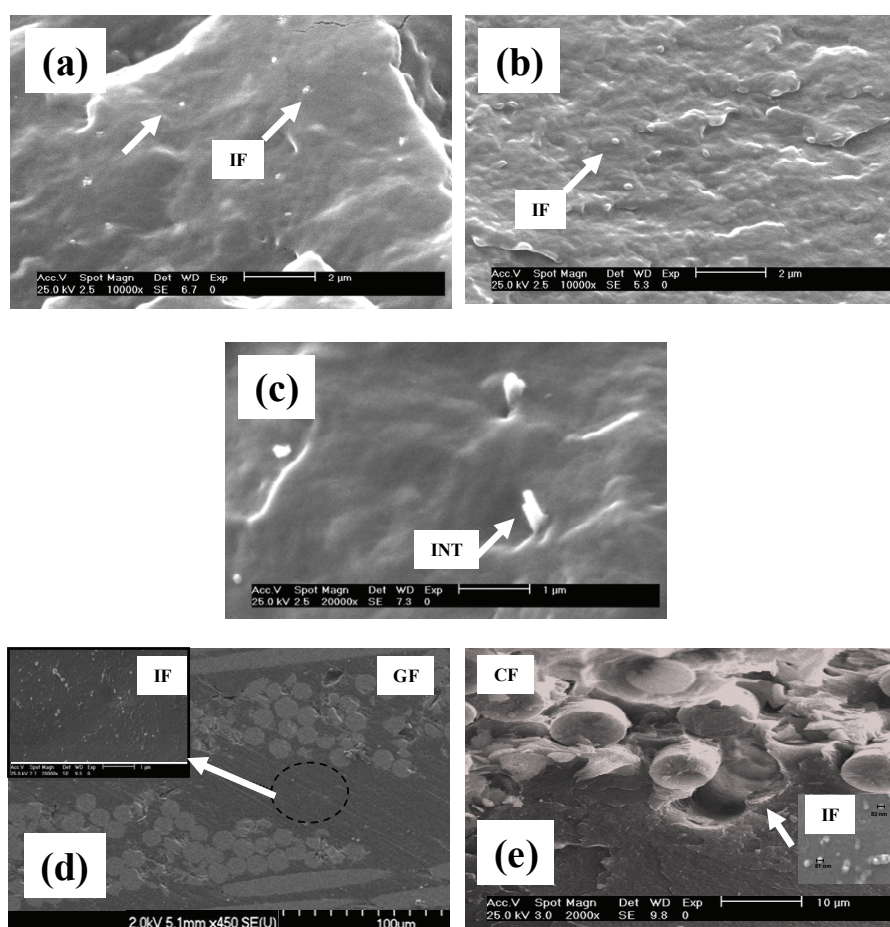
3. Thermal Properties

It is well known that the crystalline morphology and structure obtained during the thermoplastic processing plays an important role on the physico-mechanical behavior of the resulting polymeric material, conditioning its potential uses. In this way, the control of the crystallization process can be seen as a successful approach for improving physico-mechanical properties of polymers. Therefore, it is of great interest to investigate the nucleation, crystallization, and structural development of the matrix in IF/INT reinforced polymer nanocomposites [13]. This would help to optimize the manufacturing conditions in order to obtain high-performance nanocomposites and to fully exploit their potential in practical applications.

Figure 2. TGA thermograms under a nitrogen atmosphere for neat iPP, PPS and some hierarchical laminates. The inset shows the initial degradation temperature (T_i) *vs.* nanoparticle loading.
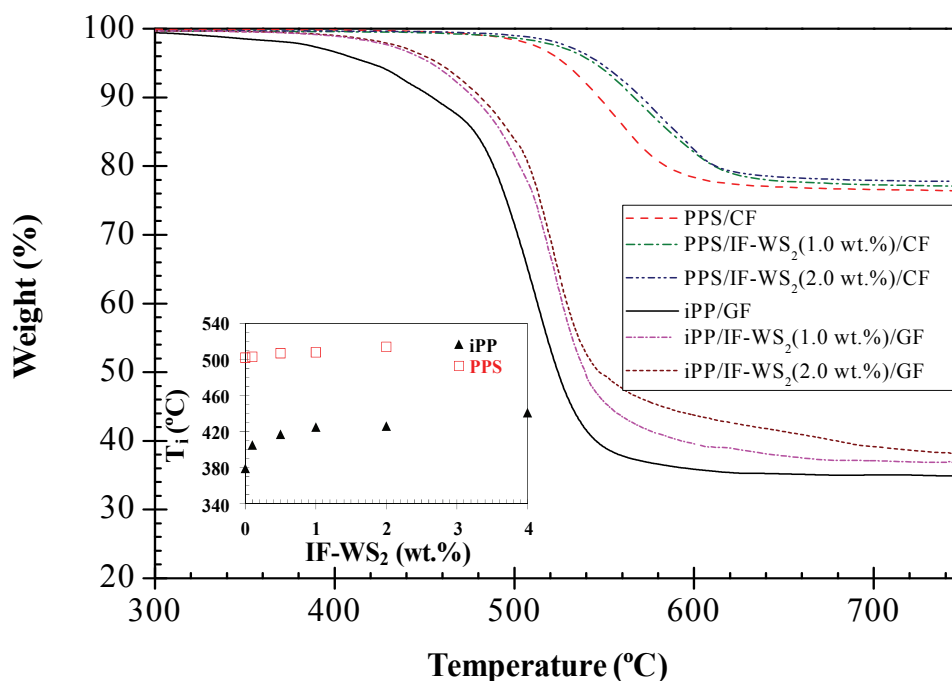
The thermal stability of several polymer matrices reinforced with IF-WS$_2$ nanoparticles was compared with that observed for other spherical inorganic nanofillers, organized by the nature of the matrix [13]. It was found that the incorporation of nanometer-sized k particles into a polymer enhances the thermal stability of the matrix inhibiting the formation and escape of volatile byproducts generated during the decomposition process. In the case of the hierarchical thermoplastic-based composites, the thermal stability of IF-WS$_2$ reinforced iPP [22] and PPS [23] laminates has been investigated using TGA, and typical thermograms under a nitrogen atmosphere for the neat matrices, and composites reinforced with 1.0 and 2.0 wt.% IF-WS$_2$ are shown in Figure 2. It is found that all the composites exhibit a single decomposition stage in a nitrogen environment, similar to that found for the neat polymers, indicating that the random scission of the polymeric chains is the predominant degradation process. The incorporation of increasing nanoparticle contents induces a progressive thermal

stabilization of both matrices (see inset of Figure 2), the effect being more significant in the case of iPP, probably related to the lower thermal stability of this commodity plastic compared to high-performance PPS. Thus, an increase in the initial degradation temperature (T_i) of 12 °C and 47 °C is attained at 2.0 wt.% loading in comparison to the reference PPS and iPP laminate, respectively. A similar trend is found for the temperature of 10% weight loss (T_{10}) and maximum rate of weight loss (T_{max}). This thermal stability enhancement has been ascribed to the barrier effect of the nanoparticles that effectively obstruct the diffusion of volatile products from the bulk of the polymer to the gas phase, therefore slowing down the decomposition process. Upon increasing IF-WS$_2$ loading, the barrier effect becomes stronger, which is reflected in higher degradation temperatures. An analogous effect of thermal stability increase has been reported for PP/GF composites reinforced with other inorganic nanoparticles such as clays [30]. Nevertheless, for the same nanofiller loading, the improvements in thermal stability are larger in the case of IF-WS$_2$, indicative of a more effective heat barrier effect of the IF nanoparticles likely arising from their more homogenous dispersion and spherical shape, thus, larger specific surface area.

In the same way, the incorporation of INTs can also lead to an improvement in the thermal stability of polymer/INTs [25,27]. As an example, the characteristic weight loss temperatures for PP nanocomposites, filled with different nanoreinforcements in nitrogen, are summarized in Table 1 [31–42]. The data reveal that the concentration of non-modified INT-MoS$_2$ has a dramatic effect on the thermal stability of the iPP nanocomposites. T_{10} of iPP/INT-MoS$_2$ (1.0 wt.%) was almost 60 °C higher than that of neat iPP, suggesting that INT-MoS$_2$ have outstanding properties for improving the thermal stability at low nanofiller content [31]. As a comparison, approximately the same increment was observed for iPP nanocomposites filled with 10 wt.% of silane-modified halloysite nanotubes (HNTs). In the case of iPP/HNTs, the thermal stability and flame-retardant effects are believed to result from the hollow tubular structure of HNTs, the barriers for heat and mass transport and the presence of iron in the HNTs [32–34]. Layered silicates, such as montmorillonite (MMT), also have important effects on the thermal stability of the PP matrix (Table 1). The dramatic improvement in thermal stability of around 90 °C was related to the confinement of the single nanoparticles in approximately 1 nm^3 volume using sophisticated methods of modification/exfoliation [39–41].

The flammability behavior of PPS/IF-WS$_2$/CF has been investigated by pyrolysis combustion flow calorimetry, in order to determine the heat release rate (HRR) at different nanoparticle contents [24]. The addition of IF-WS$_2$ leads to a progressive drop in the average peak HRR, the reduction being about 17% for the laminate with 1.0 wt.% loading. Further, the onset temperature at which begins the release of heat and the temperature at peak HRR increase gradually with the nanoparticle loading, with maximum increments of 19 and 23 °C, respectively, at 2.0 wt.% IF-WS$_2$. These improvements are probably related to the low degree of porosity and enhanced thermal stability of the hybrids. Moreover, there seems to be a synergistic effect of both micro- and nano-fillers on increasing the polymer resistance to fire. The coexistence of CFs and IF-WS$_2$ in the laminates results in a more effective confined geometry that increases the barrier resistance to the evolution of flammable volatiles. Similar synergistic behavior has been described for different polymer/clay/carbon nanotube hybrids [43,44].

Table 1. Thermal stability, crystallization, and mechanical data for isotactic polypropylene (iPP) nanocomposites using nanoreinforcing fillers with different morphologies (e.g., tubular, spherical and laminar-like particles) taken from literature. ΔT_{10} = increment of degradation temperature for 10% weight loss, ΔT_{p} = increment of crystallization peak temperature, δE = Percentage variations of Young's modulus, $\delta \sigma_y$ = Percentage variations of tensile strength and $\delta \varepsilon_b$ = Percentage variations of strain at yield.

Filler	Filler content (wt.%)	ΔT_{10} (ºC)	ΔT_{p} (ºC)	δE (GPa)	$\delta \sigma_y$ (MPa	$\delta \varepsilon_b$ (%)
INT-MoS$_2$ [31]	0.1	54	3.9	15%	13%	−9%
	0.5	59	10	28%	34%	−18%
	1	59	10.1	40%	41%	−52%
HNTs [32–34]	1	-	3.9	-	-	-
	2	-	-	32%	22%	−15%
	5	-	8.9	-	-	-
	10	60	10	-	-	-
	20	-	12.8	-	-	-
	30	46	13.8	-	-	-
CNTs [35–37]	0.1	-	7.6	-	-	-
	0.25	-	8.4	-	-	-
	0.5	-	10.7	-	-	-
	1	-	10	23%	15%	−30%
	2	50	-	-	-	-
rod-Si$_3$ N$_4$ [38]	1	-	2	722%	292%	-
	2	-	3	-	-	-
Nanoclay (MMT) [39–41]	3	90	5	152%	95%	0%
IF-WS$_2$ [16,42]	0.1	11	9.8	-	-	-
	1	14	13	39%	41%	−59%
	2	15	19	-	-	-
	4	27	20.5	-	-	-
	8	44	22.1	-	-	-

The degree of crystallinity is a key parameter in thermoplastic polymers because it has strong influence on both the chemical and mechanical properties. The crystalline phase improves the stiffness and tensile strength whilst the amorphous phase helps to absorb the impact energy. The influence of IF-WS$_2$ on the crystallization behavior of PPS/CF [23] and iPP/GF [22] has been analyzed by DSC, and typical cooling thermograms for composites with 1.0 and 2.0 wt.% loading are shown in Figure 3. Moreover, the crystallization temperature (T_p) as a function of IF-WS$_2$ concentration is plotted in the inset of this Figure. Noticeable differences are detected depending on the thermoplastic polymer. In the case of PPS based composites, the addition of low nanoparticle contents (*i.e.*, 0.1 or 0.5 wt.%) results in a decrease in T_p and the degree of crystallinity (X_c), indicating the absence of a nucleating effect of the IF-WS$_2$ on the polymer crystallization, and that the transport of macromolecular segments to the growing surface of PPS in the composite is hindered. However, the incorporation of higher

nanoparticle contents leads to an increase in both T_p and X_c, by up to 9 °C and 14%, respectively demonstrating that higher nanoparticle contents act as nucleating agents for PPS. On the other hand, these nanoparticles effectively nucleate the iPP matrix in the concentration range of 0–4.0 wt.%, with increases up to 22 °C and 6% in T_p and X_c, respectively, at the highest loading tested. These improvements are greater than those reported for binary iPP/IF-WS$_2$ nanocomposites [16], pointing towards a synergistic effect of both fillers on promoting the crystallization of iPP. This behavior is in agreement with the reported for PP/ZnO/GF [45] and PP/SiO$_2$/GF hybrids [46], where the combination of nano- and micro-fillers additionally increased the T_p of the matrix, albeit the increments found in those hybrids (~7 and 6 °C at 2.0 wt.% ZnO and 1.0 wt.% SiO$_2$ content, respectively) are smaller than the increases found for the same amount of IF-WS$_2$. Further, X_c of PP dropped upon incorporation of ZnO or SiO$_2$ and GF, while the combined nucleating effect of IF-WS$_2$/GF provoked a slight increase in crystallinity.

Figure 3. DSC crystallization thermograms for neat iPP, PPS and some IF-WS$_2$ reinforced multiscale laminates. The inset shows the crystallization peak temperature T_p *vs.* IF-WS$_2$ content.
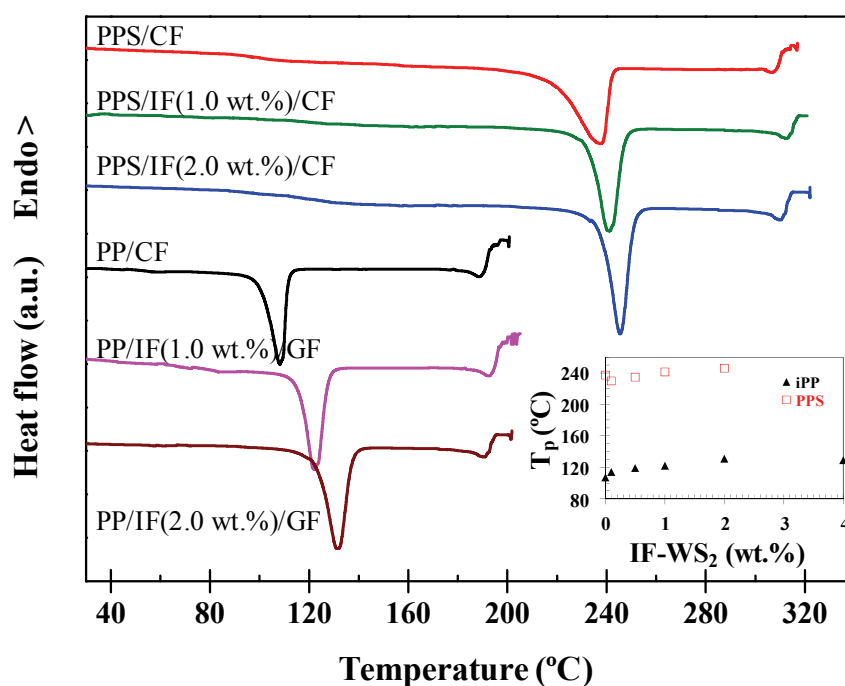
In this way, the control of the crystallization behavior has been shown to be a successful approach for improving physico-mechanical properties of polymer/INT nanocomposites. Table 1 summarizes the findings of several studies on the nucleating efficiency (NE) of nanoreinforcing fillers, and data can be compared by analyzing the difference between the crystallization peak temperature (T_p) of each nanocomposite and that of the neat matrix (ÄT$_p$). Clearly, the ÄT$_p$ value for INT-MoS$_2$ far exceeds the values observed for montmorillonite nanoclay [39] and rod-Si$_3$N$_4$ [38], and is comparable to that observed for MWCNTs [35]. However, the nucleation efficiency of INT-MoS$_2$ is significantly lower in comparison to the value of 40% observed for inorganic fullerene-like WS$_2$ nanoparticles at 1.0 wt.% [16]. The results obtained clearly show that the addition of INT-WS$_2$ plays a remarkable role in accelerating the

crystallization rate of iPP. In these systems, the crystallinity of iPP was found to rise up to 14% with increasing the INT-MoS$_2$ content, from a value of 50% for iPP, to values of 54, 57 and 56% for the nanocomposites with 0.1 wt.%, 0.5 wt.% and 1 wt.%, respectively [25]. Furthermore, a new study on the crystallization behavior of biopolymer/INTs suggests that INT-WS$_2$ exhibits much more prominent nucleation activity on the crystallization of PHB than other specific nucleating agents or nano-sized fillers [29]. An increment of 35 °C in the crystallization temperature of PHB was observed for as little as 0.1 wt.% INT-WS$_2$. This corresponds to the highest value observed hitherto for PHB formulations using specific nucleating agents (e.g., talc, boron nitride lignin) or nano-sized fillers (e.g., CNTs, graphene oxide) [29].

Figure 4. Room temperature thermal conductivity of iPP and PPS-based laminates as a function of IF-WS$_2$ concentration.
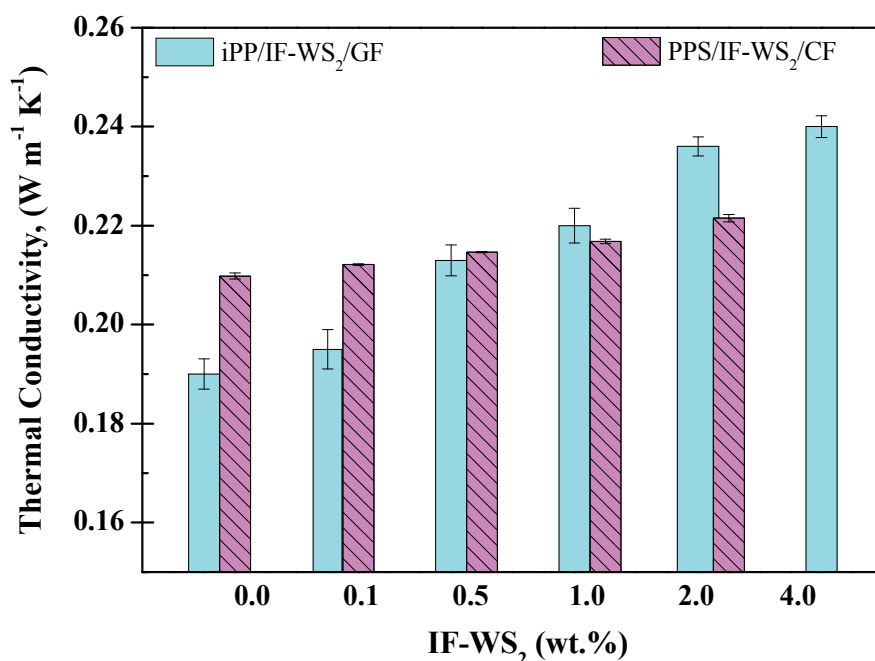

The addition of thermally conductive organic or inorganic nanofillers typically enhances the thermal conductivity (λ) of polymers, which is interesting for applications that require effective dissipation of accumulated heat like connectors or thermal interface materials. It depends on several factors, namely the filler size, aspect ratio, concentration and state of dispersion, the nature, molecular weight and degree of crystallinity of the polymer, as well as the porosity of the material. The room temperature thermal conductivity of iPP- [22] and PPS- [24] based laminates has been measured in the transverse directions, and the results are shown in Figure 4. The incorporation of IF-WS$_2$, which exhibit about twice the thermal conductivity of the neat matrices [47], results in significant λ improvements in the case of iPP/GF laminates, up to 21% at 2.0 wt.% loading, whilst for PPS/CF composites the increments are smaller, about 9% for the same loading. This discrepancy is ascribed to the low thermal conductivity of the GF fabric (~0.05 W m^{-1} K^{-1}) compared to that of CF (>200 W m^{-1} K^{-1}). It seems that the CFs play a dominating role in the thermal conductivity properties and mask the effect of the IF-WS$_2$, as can be deduced from the comparison with the results of binary PPS/IF-WS$_2$ nanocomposites [48], where λ rose by up to ~45% upon addition of 2.0 wt.% IF-WS$_2$. However, for iPP-based samples, the

improvements in the hierarchical laminates are comparable to those reported for the corresponding binary composites [49], indicating that effect of the nanoparticles predominates. An analogous behavior has been reported for other hierarchical laminates based on thermoplastic polymers, such as PEEK/CNT/GF laminates [50], where λ increased by ~48% at 1.0 wt.% CNT, similarly to the enhancements found in the binary composites [51]. It is worthy to note that for the same nanofiller concentration, the increases in λ upon addition of CNTs are only about double those achieved with the incorporation of the IF-WS$_2$, while much higher differences would be expected considering the extraordinary high thermal conductivity of CNTs. The strong agglomerating tendency of CNTs, the small thermal conductance of the nanotube-polymer interface and the high interfacial thermal resistance between nanotubes within a bundle probably limits the property enhancement, whereas for composites incorporating IF-WS$_2$ the large nanofiller-matrix interfacial contact area and the very homogeneous dispersion lead to experimental λ values even higher than the theoretical predictions.

4. Mechanical Properties

The dynamic mechanical properties of the multiscale composites were explored by DMA, technique that provides information about the viscoelastic behavior of the matrix, indicating changes in the stiffness and the relaxation processes that occur as a function of temperature. The influence of the IF-WS$_2$ on the dynamic mechanical behavior of polymer/IF-WS$_2$ nanocomposites has also been investigated [16–18]. In particular, it was observed that the improvements in the storage modulus values of PPS/IF-WS$_2$ nanocomposites are noticeably higher than those achieved in other thermoplastic nanocomposites based on IFs (e.g., iPP, nylon-6, PEEK), suggesting the presence of specific polymer-filler interactions in the case of PPS. The molecular nature of these interactions are still not understood, but they may be associated with the presence of outer S atoms on the IF nanoparticles, and more work is required in order to explain this phenomenon. Figure 5 presents the storage modulus (E') and loss tangent (tan δ) at the frequency of 1 Hz for PPS- and iPP-based composites incorporating 1.0 and 2.0 wt.% IF-WS$_2$, and the glass transition temperature (T_g) *vs.* nanoparticle content is shown in the inset of the Figure. Different behavior is also observed depending on the polymer matrix. Regarding PPS/CF laminates, the addition of very low IF-WS$_2$ loadings (*i.e.*, 0.1 wt.%) leads to a slight drop in E' (~7% at 25 °C), probably related to the decrease in the crystallinity found for this sample, as revealed by DSC analysis, since the crystalline regions enhance the modulus of semicrystalline polymers. The laminate incorporating 0.5 wt.% IF-WS$_2$ exhibits similar E' to that of PPS/CF, since the reinforcement effect of the IF-WS$_2$ should compensate for the slight decrease in crystallinity. In contrast, the incorporation of nanoparticle contents > 0.5 wt.% leads to significant E' increments, by up to 22% for 2.0 wt.% nanoparticle content at 25 °C. On the other hand, the gradual addition of IF-WS$_2$ to iPP/GF results in progressive E' increases, by about 27% at 2.0 wt.% loading. This behavior is associated with the increase in crystallinity caused by heterogeneous nucleation, combined with an effective reinforcement effect arising from a very homogeneous nanoparticle dispersion. For both types of composites, the reinforcement effect is more pronounced at temperatures below T_g, in agreement with the behavior reported for PP/nanoclay/GF composites [30], where significant E' enhancements were found at low temperatures whereas the differences in modulus among the samples became insignificant at temperatures above the glass transition.

Figure 5. Evolution of the (**a**) storage modulus E' and (**b**) tan δ as a function of temperature for the neat polymers and some multiscale laminates. The inset shows the glass transition temperature T_g *vs.* IF-WS$_2$ content.
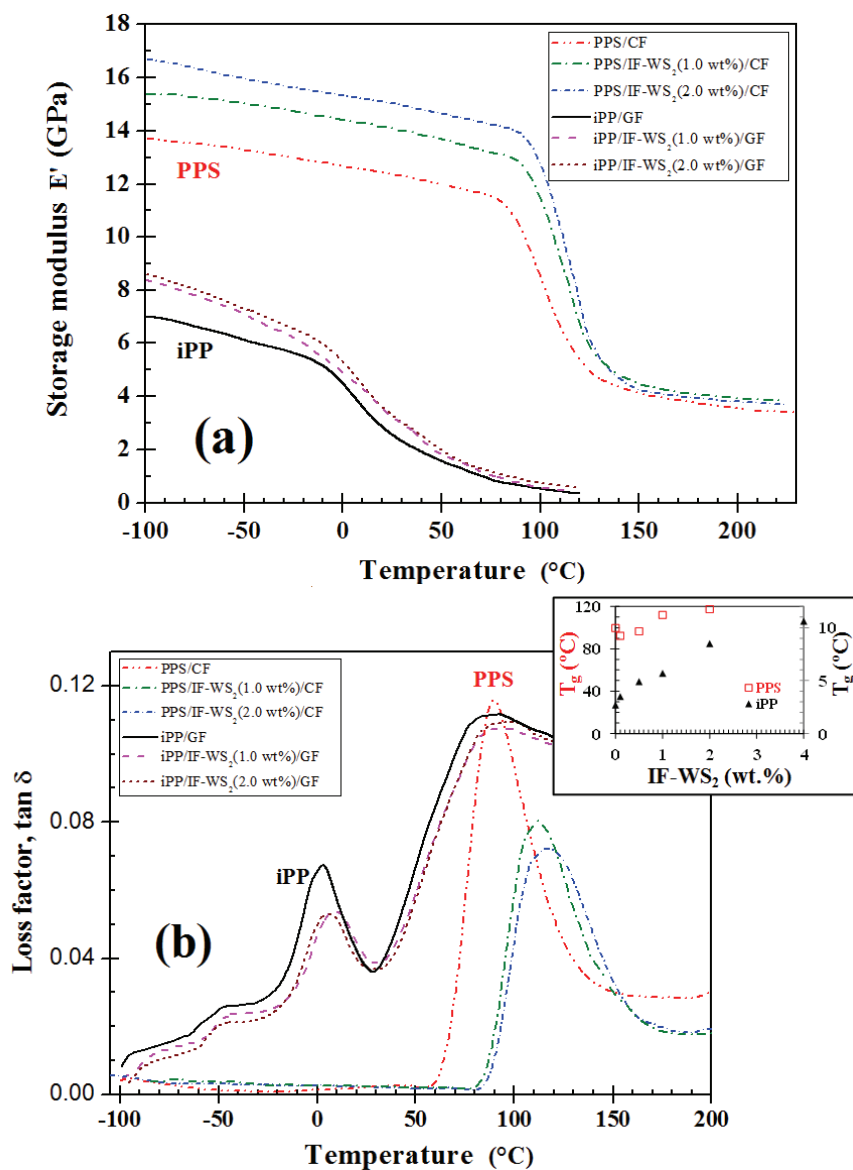
The evolution of tan δ (ratio of the loss to storage modulus, a measure of the damping within the system) as a function of temperature (Figure 5b) exhibits an intense peak, named α relaxation that corresponds to the T_g. Further, the iPP/GF laminates show a peak at about 88 °C related to the relaxation of the crystalline phase (α$_c$). In an unfilled system, the polymer chain segments are free from restraints. The incorporation of fillers decreases the free volume and restricts the mobility of the matrix chains, which is reflected in higher T_g values (see inset of Figure 5). Once again, different trend is found depending on the nature of the matrix. Thus, in the case of PPS/CF, the incorporation of low IF-WS$_2$ contents (≤ 0.5 wt.%) led to a downshift in T_g, while the addition of higher concentrations resulted in an upshift. As mentioned above, the addition of low nanoparticle loadings slows down the crystallization rate of PPS, leading to the formation of a more amorphous phase that provokes a slight drop in T_g. However, the incorporation of higher contents has a nucleation effect, thereby raising the

crystallinity of the polymer, which combined with a larger IF-WS$_2$-matrix interfacial contact area results in an effective immobilization of the polymer chains, consequently an increase in T_g of up to 18 °C at 2.0 wt.% IF-WS$_2$. In contrast, the T_g progressively increases upon addition of these nanoparticles to iPP/GF, the increment being about 6 °C for the same nanoparticle loading. In the same way, the presence of IF-WS$_2$ causes an increase in the crystalline relaxation temperature α_c of iPP, since the strong nucleation effect of these nanoparticles accelerates the crystallization of iPP in the nanocomposites.

The magnitude of the tan δ peak is indicative of the filler-matrix interactions. For both types of composites, the height of the tan δ peak decreases with increasing IF-WS$_2$ content, indicative of a strong nanofiller-matrix interfacial adhesion. Moreover, this reduction probably arises from a synergistic effect between the micro- and nano-fillers on restricting chain mobility, in agreement with the behavior reported for other GF-reinforced hierarchical composites [52]. The incorporation of both reinforcements has a strengthening effect, leading to a lower degree of molecular motion, hence, lower damping characteristics. It also noteworthy that the width of the tan δ peak becomes broader with increasing nanoparticle loading, phenomenon that can be interpreted as improved nanofiller-matrix interactions, and is another indication of the larger nanoparticle-matrix interfacial area. The IF-WS$_2$ and microscale fibers disturb the relaxation of the neighbour polymer chains, which would behave differently from those situated in the bulk matrix, resulting in a wider maximum. This behavior was also observed in IF-WS$_2$ reinforced iPP [16] and PEEK [18] nanocomposites, attributed to a more inhomogeneous amorphous phase in the composites in relation to the pure matrix.

The static mechanical properties of iPP and PPS based hybrid laminates have been investigated by tensile tests [22,23], and the Young's modulus (E), tensile strength (σ_y), elongation at break (ε_b), and toughness (T) as a function of nanofiller loading are plotted in Figure 6. The trends observed are similar to those described previously for the storage modulus. E and σ_y rise progressive with increasing nanoparticle loading in the case of iPP/GF composites, while they decrease slightly at low loadings and then grow in PPS/CF laminates, behavior that is directly related to the crystallinity of the samples, as discussed previously. Interestingly, both parameters only rise marginally upon addition of the IF-WS$_2$, the maximum increments being ~14% and 11% at 2.0 wt.% nanoparticle content, respectively, in the case of PPS/CF, and even smaller for iPP/GF composites (Figure 6). However, considerably larger increases were observed for the binary iPP/IF-WS$_2$ nanocomposites [49], where E and σ_y improved by around 42 and 31%, respectively, for the indicated loading. For multiscale composites, it is expected that the nanofillers predominantly influence the properties that are matrix-dominated; consequently, only small increases are observed in the Young's modulus and tensile strength of the hybrids, since the tensile properties are more fiber-dominated. These results are consistent with the behavior reported for other thermoplastic-based hybrids [53], where E and σ_y of the fiber reinforced polymer only improved marginally upon incorporation of the nanoscale fillers due to the dominating role of the fibers.

With regard to the strain at break (ε_b), the trend found is very similar for both composite series. A moderate increase is found at low nanoparticle loadings, followed by a sharp reduction at higher concentrations. This indicates that higher amounts of IF-WS$_2$ hinder the ductile flow of the matrix. This tendency is in contrast to that typically reported for CNT-reinforced multiscale laminates [53], where ε_b systematically decreases upon addition of the carbon nanofillers, attributed to the presence of aggregates that produces stress concentrations at the filler-matrix interface, leading to premature failure. Similarly, Rahman *et al.* [30] found around 50% reduction in tensile strain upon incorporation

of 6.0 wt.% nanoclay to PP/GF (30 wt.%), also ascribed to the poor nanoclay dispersion that strongly limits the plastic deformation of the matrix. The surprising behavior observed for the composites filled with IF-WS$_2$ is probably related to the lubricant character and more uniform dispersion of these inorganic nanoparticles combined with their spherical shape that reduce the stress concentration sites, thereby improving the matrix ductility. However, for IF-WS$_2$ concentrations higher than 1.0 wt.%, a stiff hybrid network of micro- and nano-fillers could be formed that acts very effectively as a barrier for the mobility of the polymer chains, thus limiting the ductile deformation. A qualitatively similar behavior is found for the toughness, measured as the area under the tensile curve, that increases considerably at low IF-WS$_2$ loadings (*i.e.*, by 35% at 0.1 wt.% content compared to iPP/GF) while drops moderately at concentrations higher than 1.0 wt.% (around 20% decrease at 2.0 wt.% loading compared to PPS/CF). The small aggregates contribute to increase the brittleness under high strain rates, since they nucleate secondary cracks and favour the formation of dimples.

Figure 6. (**a**) Young's modulus (*E*), (**b**) tensile strength (σ_y), (**c**) elongation at break (ε_b) and (**d**) toughness (*T*) as a function of IF-WS$_2$ loading. Solid and open symbols correspond to PPS/IF-WS$_2$/CF and iPP/IF-WS$_2$/GF systems, respectively.
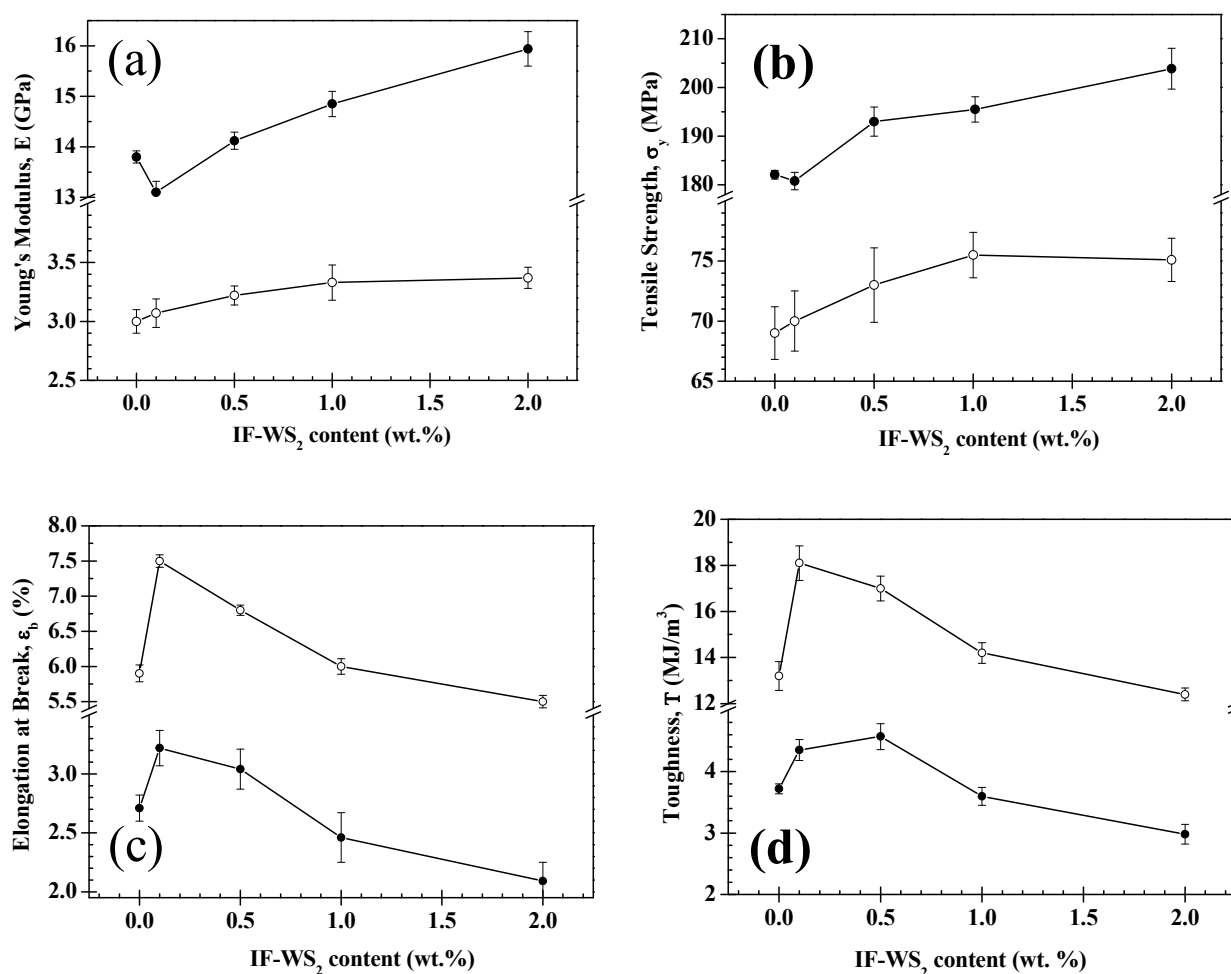
The influence of the IF-WS$_2$ on the flexural properties of iPP/GF and PPS/CF has also been investigated [22,24]. In this case, maximum increments in the flexural modulus E_f and flexural strength

σ_{fM} of iPP/GF up to 26 and 22%, respectively, have been attained at 2.0 wt.% loading. Similarly, enhancements of 25 and 15% have been found in PPS/CF composites for the same nanofiller loading. The comparison of the results with those obtained for the corresponding binary nanocomposites [22,24] reveals a synergistic effect of both fillers on enhancing the flexural properties of the matrix.

Table 2. Comparison of the increment in static mechanical properties (in %) for different polypropylene (PP) and polyphenylene sulfide-(PPS) based hierarchical laminates. MWCNT: multi-walled carbon nanotubes; MMT: montmorillonite; Woll: Wollastonite; E: Young's modulus; σ_y: tensile strength at yield; G: impact strength; E_f: flexural modulus; σ_{fM}: flexural strength.

Matrix	Fiber (wt.%)	CNT (wt.%)	ΔE (%)	$\Delta\sigma_y$ (MPa)	ΔT (%)	ΔE_f (%)	$\Delta\sigma_{fM}$ (%)	Ref.
PP	GF (5)	MWCNTs	40	39	24	36	43	[18]
PP	CF (5)	MWCNTs	57	37	34	51	35	[18]
PP	GF (30)	MMT (6)	6	6	-	9	10	[3]
PP	GF (30)	Woll (10)	−6	−6	−31	−2	−3	[19]
PP	GF (40)	SiO_2 (1)	22	3	−5	2	12	[9]
PP	GF (30)	IF-WS$_2$ (2)	10	8	-	26	22	[1]
PPS	GF (40)	$CaCO_3$ (3 wt.%)	27	9	14	-	-	[20]
PPS	GF (40)	$CaCO_3$ (3)	-	-	20	0	3	[21]
PPS	CF	IF-WS$_2$ (2)	14	11	−20	25	15	[2,4]

Table 2 compares the improvements in static mechanical properties reported for various PP and PPS-based hierarchical composites [30,46,54–57]. Clearly, the highest improvements are attained upon addition of multi-walled carbon nanotubes (MWCNTs) to fiber-reinforced PP composites [54], which is reasonable taking into account the very high modulus of these carbon nanofillers. Nevertheless, among the various inorganic fillers, IF-WS$_2$ lead to larger stiffness and strength improvements than montmorillonite [30], wollastonite [55], or nanosilica [46], and comparable to those of CaCO$_3$ [56,57].

In the same way, the incorporation of INTs can also lead to improvement in the mechanical properties of polymer/INTs [25,27]. As an example, the characteristic mechanical data (e.g., Young's modulus, E, tensile strength, σ_y and strain at yield, ε_y) for the PP nanocomposites incorporating nanoreinforcing fillers with different morphologies are summarized in Table 1 [31–42]. It can be observed that the addition of INT-MoS$_2$ progressively enhances the Young's modulus of the matrix, with increments of 15, 28, and 40% for loading fractions of 0.1, 0.5, and 1.0 wt.%, respectively. The improved E obtained in this work is ascribed to the very uniform dispersion of the INT-MoS$_2$ and their

high aspect ratio, which results in larger nanofiller-polymer interfacial area. Qualitatively similar trends were found for the tensile strength, where the increments were around 13, 34, and 41% for the abovementioned nanofiller contents. On the other hand, the incorporation of the inorganic nanotubes leads to a slight decrease in ε_y. This is a typical behavior of nanofiller-reinforced polymer composites, since the nanofillers restrict the ductile flow of the matrix, and is in agreement with the results reported by Lopez-Gaxiola *et al*. [58] for carbon filler-reinforced PP composites. Table 1 also shows the percentage variations in the mechanical properties of iPP nanocomposites containing similar amounts (~1.0 wt.%) of various nanofillers. Remarkable improvements in the mechanical properties are observed for iPP/INT-MoS$_2$, where the non-modified nanofillers were dispersed uniformly in the iPP matrix for all the compositions prepared [31]. The magnitude of increase in the modulus and strength is similar to that obtained for IF-WS$_2$ nanoparticles [42] and far exceeds that reported for both modified HNTs [34] and CNTs [37]. However, silicon nitrides clearly provide the best reinforcement for PP matrix, which has been related to the alignment and exfoliation of rod-shaped Si$_3$N$_4$ particles [38]. These phenomena were also mainly responsible for the 95% enhancement in the tensile strength and 152% increase in the tensile modulus of PP using p-aminobenzoic acid modified-clay with PP-g-MA as a compatibilizer [40]. On the other hand, Reddy *et al*. have reported that the high rigidity of INT-WS$_2$ and the effective load transfer from the matrix to the INT-WS$_2$ were responsible for the improved mechanical properties of PMMA/INT-WS$_2$ nanocomposites [27]. In particular, it was observed that the elastic modulus of PMMA fiber meshes was increased by 10 and 22 times upon incorporation along the fiber axis of 1.0 and 2.0 wt.% INT-WS$_2$, respectively. Analogously, the tensile strength of the composite fibers increased by 35 and 32% for the indicated nanoparticle loadings. However, the toughness of the sample with 2.0 wt.% INT-WS$_2$ was lower than that of the neat PMMA fiber, since nanofiller aggregation started to take place. Overall, experimental results point out the advantages of using these environmentally friendly and cheap inorganic fullerenes and nanotubes instead of conventional nanoparticles for improving the mechanical performance of thermoplastic composites.

5. Tribological Properties

Inorganic nanoparticles are frequently incorporated into thermoplastic polymers with the aim to improve the tribological properties. The nanoparticles exhibit some advantages compared to conventional microfillers, such as higher specific surface area, lower abrasiveness due to a reduced angularity, enhanced strength, modulus and toughness. In addition, IF-WS$_2$ possess a lubricant character, and have been shown to be effective for improving the tribological properties of thermoplastic polymers such as PPS or PEEK [59,60]. Figure 7 displays the change in the coefficient of friction (μ) and wear rate of PPS/CF upon addition of IF-WS$_2$ [23]. The incorporation of 0.1 wt.% IF-WS$_2$ leads to a slight increase in μ (~5%) compared to the reference laminate, probably related to the decrease in stiffness and strength found for this sample that prevails over the lubricant effect of the IF-WS$_2$. Further increasing the nanoparticle loading, μ drops strongly, reaching the lowest value at 2.0 wt.% IF-WS$_2$ (about 32% drop compared to the reference laminate). Rapoport *et al*. [61] proposed a rolling mechanism for these nanoparticles, in which they act as a ball-bearing component, implying that they roll instead of sliding between the surfaces, hence, decreasing the shear stress, contact temperature and coefficient of friction. Likewise, the abovementioned behavior can be attributed to a

synergistic effect between the CFs and the inorganic nanoparticles, as reported previously for CF-reinforced PEEK incorporating ZnS or TiO_2 nanoparticles [62].

Figure 7. Coefficient of friction and wear rate of PPS/IF-WS$_2$/CF laminates as a function of IF-WS$_2$ content.
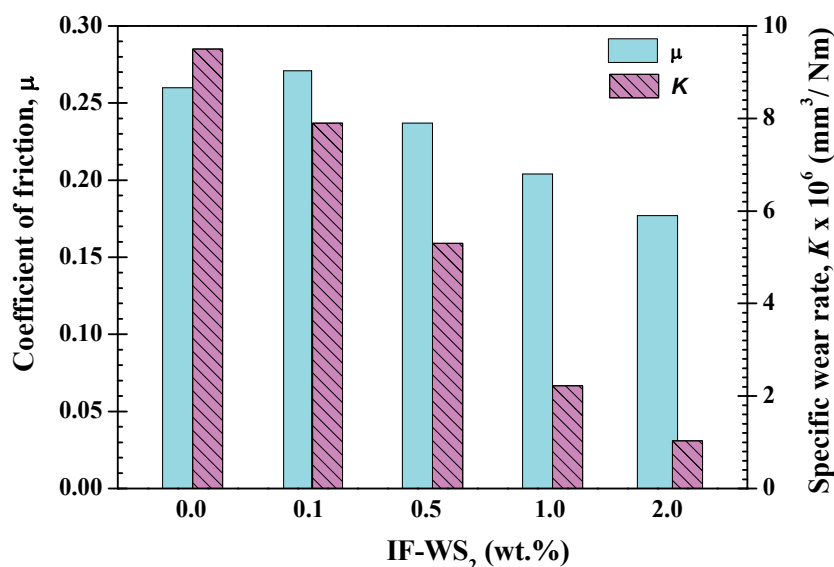
With regard to the wear rate, a progressive reduction in this parameter is found upon increasing IF-WS$_2$ concentration, which decreases by nine-fold for the composite with 2.0 wt.% loading compared to the reference laminate. This increase in wear resistance has been attributed to the formation of a thin, continuous, and smooth transfer film on the counterface during sliding combined with the reinforcing effect, and it is enhanced by the presence of the two fillers. The adhesion of the transfer film would be stronger since a homogeneous mixture of the debris is formed, and the resistance to cracking and fatigue failure would also increase in the presence of the nanoparticles. An analogous trend was reported for the wear behavior of PEEK/ZrO$_2$/CF composites [62], where a synergistic effect of CFs with ZrO$_2$ nanoparticles on enhancing the matrix wear resistance was proposed. Overall, the combination of conventional CF-reinforced thermoplastics with lubricant nanoparticles like IF-WS$_2$ is a promising approach to develop multiscale hybrids with superior tribological performance.

Table 3. Wear rate (K) data of PP nanocomposites nanocomposites using nanoreinforcing fillers with different morphologies.

Filler	Filler content (wt.%)	Wear rate $(K) \times 10^4$ (mm^3/Nm)	Percentage variation of K (%)
INT-MoS$_2$	0	6.27	-
[31]	0.1	5.97	5
	0.5	4.35	31
	1	2.98	53
Nanoclay [65]	1	-	38.5
IF-WS$_2$ [42]	1	-	63

Table 3 collects the wear rate of melt-procesable iPP/INT-MoS$_2$ nanocomposites [31]. With the incorporation of INT-MoS$_2$ the wear resistance of the polymer is considerably enhanced and the nanocomposite with 1.0 wt.% loading shows a reduction of about 53%. These inorganic nanotubes dispersed in the polymer matrix can act as a barrier and prevent large-scale fragmentation of the iPP. It has been reported that nanofillers of similar dimensions as the segments of the surrounding polymer chains enable a milder material removal and aid the formation of uniform tenacious transfer film [63,64]. Table 3 also compares the percentage of variations in the wear rate of PP nanocomposites containing 1.0 wt.% of nanoclay [65], IF-WS$_2$ [42], and INT-MoS$_2$ [31]. In particular, PP/INT-MoS$_2$ showed higher wear property improvement than that of PP/nanoclay without the need for an exfoliation process. The highest percentage of improvement in wear rate is found for IF-WS$_2$ solid lubricant nanoparticles, which have recently been identified as ideal candidates for improving the tribological performance of polymers like epoxy [61], nylon-6 [19], and PEEK [18].

6. Conclusions and Future Developments

The addition of IF/INTs has been demonstrated to be a very efficient strategy to improve the thermal, mechanical and tribological properties of thermoplastic polymers like iPP, PPS, or PEEK and their fiber-reinforced composites. These materials can be fabricated by simple melt-processing and compression molding without the need for modifiers or surfactants, leading to a very homogenous dispersion of the nanofillers within the matrix. More importantly, they exhibit similar or enhanced performance when compared with composites that incorporate CNTs, nanoclays or other inorganic spherical nanoparticles, but are substantially more cost-effective, efficient and environmentally-friendly. Results demonstrate the existence of synergistic effects of both micro-and nanoscale fillers on enhancing the stiffness, strength, thermal conductivity, thermal stability, flammability, and wear resistance of hierarchical thermoplastic-based composites. This new family of materials has a wide range of potential applications ranging from medicine to the aerospace, automotive, and electronics industries. Some of these applications are still at an early stage of research and development. However, for optimal control of the properties of these new materials, it is highly important to tailor the fabrication process from the viewpoint of the final product. In particular, the improvement and application of these nanocomposites in comparison with other organic-inorganic hybrid nanomaterials (silica, metal oxides, clays, *etc*.) depend on how effectively we optimize and scale-up their fabrication method. For specific applications, these nanoparticles should be surface functionalized in order to confer more selectivity, specificity and reactivity with the polymer chains. An additional demanding area is the potential of these nanoparticles in the field of biocompatible and/or biodegradable polymeric composites for packaging and medical applications and their eventual toxicological effects, if any, need to be investigated. Research and progress in these areas will not only benefit the current applications but would also lead to new markets as well as to future development of diverse hierarchical thermoplastic-based composites.

Acknowledgments

Author Contributions

This project was conceived and designed by MN. AD characterized and discussed the mechanical and tribological properties. MN analyzed and discussed the morphology and thermal properties. Both authors contributed in writing this paper.

Conflicts of Interest

The authors declare no conflict of interest.

References

1. Offringa, A.R. Thermoplastic composites in aerospace-proven through cost-effective processing. In Proceedings of the 41th International Conference on Automated Composites (ICAC), Nottingham, UK, 6–7 September 1995.
2. Henshaw, J.M.; Han, W.J.; Owens, A.D. An overview of recycling issues for composite materials. *J. Thermoplast. Compos. Mater.* **1996**, *1*, 4–20.
3. Marsh, G. Next step for automotive materials. *Mater. Today* **2003**, *6*, 36–43.
4. Sanchez, C.; Belleville, P.; Polpall, M.; Nicole, L. Applications of advanced hybrid organic-inorganic nanomaterials: From laboratory to market. *Chem. Soc. Rev.* **2011**, *40*, 696–753.
5. Qian, H.; Greenhalgh, E.S.; Shaffer, M.S.P.; Bismarck, A. Carbon nanotube-based hierarchical composites: A review. *J. Mater. Chem.* **2010**, *20*, 4751–4762.
6. Lin, G.; Xie, G.; Sui, G.; Yang, R. Hybrid effect of nanoparticles with carbon fibers on the mechanical and wear properties of polymer composites. *Compos. Part B* **2012**, *43*, 44–49.
7. Hussain, M.; Nakahira, A.; Nishijima, S.; Niihara, K. Evaluation of machanical behaviour of CFRC transverse to the fiber direction at room and cryogenic temperature. *Compos. Part A* **2000**, *31*, 173–179.
8. Timmerman, J.F.; Hayes, B.S.; Seferis, J.C. Nanoclay reinforcement effects on the cryogenic microcraking of carbon fiber/epoxy composites. *Compos. Sci. Technol.* **2002**, *62*, 1249–1258.
9. Tenne, R. Inorganic nanotubes and fullerene-like nanoparticles. *Nat. Nanotechnol.* **2006**, *1*, 103–111.
10. Tenne, R.; Redlich, M. Recent progress in the research of inorganic fullerene-like nanoparticles and inorganic nanotubes. *Chem. Soc. Rev.* **2010**, *39*, 1423–1434.
11. Tenne, R.; Margulis, L.; Genut, M.; Hodes, G. Polyhedral and cylindrical structures of WS_2. *Nature* **1992**, *360*, 444–445.
12. Margulis, L.; Salitra, G.; Tenne, R.; Talianker, M. Nested fullerene-like structures. *Nature* **1993**, *365*, 113–114.

13. Naffakh, M.; Díez-Pascual, A.M.; Marco, C.; Ellis, G.; Gómez-Fatou, M.A. Opportunities and challenges in the use of inorganic fullerene-like nanoparticles to produce advanced polymer nanocomposites. *Prog. Polym. Sci.* **2013**, *38*, 1163–1231.

14. Kickelbick, G. Concepts for the incorporation of inorganic building blocks into organic polymers on a nanoscale. *Prog. Polym. Sci.* **2003**, *28*, 83–114.

15. Rozenberg, B.A.; Tenne, R. Polymer-assisted fabrication of nanoparticles and nanocomposites. *Prog. Polym. Sci.* **2008**, *33*, 40–112.

16. Naffakh, M.; Martin, Z.; Fanegas, N.; Marco, C.; Gómez, M.A.; Jiménez, I. Influence of inorganic fullerene-like WS$_2$ nanoparticles on the thermal behavior of isotactic polypropylene. *J. Polym. Sci. B* **2007**, *45*, 2309–2321.

17. Naffakh, M.; Marco, C.; Gómez, M.A.; Gómez-Herrero, J.; Jiménez, I. Use of inorganic fullerene-like WS$_2$ to produce new high-performance polyphenylene sulfide nanocomposites: Role of the nanoparticle concentration. *J. Phys. Chem. B* **2009**, *113*, 10104–10111.

18. Naffakh, M.; Díez-Pascual, A.M.; Marco, C.; Gómez, M.A.; Jiménez, I. Novel melt-processable poly(ether ether ketone) (PEEK)/inorganic fullerene-like WS$_2$ nanoparticles for critical applications. *J. Phys. Chem. B* **2010**, *114*, 11444–11453.

19. Naffakh, M.; Marco, C.; Gomez, M.A.; Jimenez, I. Novel melt-processable nylon-6/inorganic fullerene-like WS$_2$ nanocomposites for critical applications. *Mater. Chem. Phys.* **2011**, *129*, 641–648.

20. Naffakh, M.; Marco, C.; Ellis, G. Novel polypropylene/inorganic fullerene-like WS$_2$ nanocomposites containing a β-nucleating agent: Dynamic crystallization and melting behaviour. *J. Phys. Chem. B* **2011**, *115*, 10836–10843.

21. Naffakh, M.; Díez-Pascual, A.M.; Gómez-Fatou, M.A. New hybrid nanocomposites containing carbon nanotubes, inorganic fullerene-like WS$_2$ nanoparticles and poly(ether ether ketone) (PEEK). *J. Mater. Chem.* **2011**, *21*, 7425–7433.

22. Díez-Pascual, A.M.; Naffakh, M. Tuning the properties of carbon fiber-reinforced poly(phenylene sulphide) laminates via incorporation of inorganic nanoparticles. *Polymer* **2012**, *53*, 2369–2378.

23. Díez-Pascual, A.M.; Naffakh, M. Polypropylene/glass fiber hierarchical composites incorporating inorganic fullerene-like nanoparticles for advanced technological applications. *ACS Appl. Mater. Interfaces* **2013**, *5*, 9691–9700.

24. Díez-Pascual, A.M.; Naffakh, M. Inorganic nanoparticle-modified carbon fiber fabric/poly(phenylene sulphide) laminates with enhanced thermomechanical behaviour. *Materials* **2013**, *6*, 3171–3193.

25. Naffakh, M.; Remškar, M.; Marco, C.; Gómez, M.A.; Jiménez, I. Towards a new generation of polymer nanocomposites based on inorganic nanotubes. *J. Mater. Chem.* **2011**, *21*, 3574–3578.

26. Zohar, E.; Baruch, S.; Shneider, M.; Dodiu, H.; Kenig, S.; Wagner, D.H.; Zak, A.; Moshkovith, A.; Rapoport, L.; Tenne, R. The Mechanical and Tribological Properties of Epoxy Nanocomposites with WS$_2$ Nanotubes. *Sens. Transducers J.* **2011**, *12*, 53–65.

27. Reddy, C.S.; Zak, A.; Zussman, E. WS$_2$ nanotubes embedded in PMMA nanofibers as energy absorptive material. *J. Mater. Chem.* **2011**, *21*, 16086–16093.

28. Lalwani, G.; Henslee, A.M.; Farshid, B.; Parmar, P.; Lin, L.; Qin, Y.X.; Kasper, F.K.; Mikos, A.G.; Sitharaman, B. Tungsten disulfide nanotubes reinforced biodegradable polymers for bone tissue engineering. *Acta Biomater.* **2013**, *9*, 8365–8373.

29. Naffakh, M.; Marco, C.; Ellis, G. Inorganic WS$_2$ Nanotubes that improve the crystallization behavior of biodegradable poly(3-hydroxybutyrate). *Cryst. Eng. Comm.* **2013**, *16*, 1126–1135.

30. Rahman, N.A.; Hassan, A.; Yahya, R.; Lafia-Araga, R.A.; Hornsby, P.R. Polypropylene/glass fiber/nanoclay hybrid composites: morphological, thermal, dynamic mechanical and impact behaviors. *J. Reinf. Plast. Compos.* **2012**, *31*, 269–281.

31. Naffakh, M,.; Díez-Pascual, A.M.; Remškar M, Marco, C. New inorganic nanotube polymer nanocomposites: Improved thermal, mechanical and tribological properties in isotactic polypropylene incorporating INT-MoS$_2$. *J. Mater. Chem.* **2012**, *22*, 17002–17010.

32. Liu, M.; Guo, B.; Du, M.; Chen, F.; Jia, D. Halloysite nanotubes as a novel β- nucleating agent for isotactic polypropylene. *Polymer* **2009**, *50*, 3022–3030.

33. Du, M.; Guo, B.; Jia, D. Thermal stability and flame retardant effects of halloysite nanotubes on polypropylene. *Eur. Polym. J.* **2006**, *42*, 1362–1369.

34. Prashantha, K.; Lacrampe, M.F.; Krawczak, P. Processing and characterization of alloysite nanotubes filled polypropylene nanocomposites based on a masterbatch route: Effect of halloysites treatment on structural and mechanical properties. *Express Polym. Lett.* **2011**, *5*, 295–307.

35. Marco, C.; Naffakh, M.; Gómez, M.A.; Santoro, G.; Ellis, G. The crystallization of polypropylene in multiwall carbon nanotube based composites. *Polym. Compos.* **2011**, *32*, 324–333.

36. Jin, S.H.; Kang, C.H.; Yoon, K.H.; Bang, D.S.; Park, Y.B. Effect of compatibilizer on morphology, thermal and rheological properties of polypropylene/functionalized multi-walled carbon nanotubes composite. *Appl. Polym. Sci.* **2009**, *111*, 1028–1033.

37. Lui, Y.; Gao, J. Mechanical properties and wear behavior of polypropylene/carbon nanotube nanocomposites. *Adv. Mater. Res.* **2011**, *798*, 299–300.

38. Rangari, V.K.; Shaik, Y.M.; Mohammad, G.M.; Jeelani, S. Reinforcement of Si$_3$N$_4$ nanoparticles in Polypropylene single fibers through melt extrusion process and their properties. *J. Appl. Polym. Sci.* **2011**, *121*, 1512–1520.

39. Xu, W.; Ge, M.; He, P. Nonisothermal crystallization kinetics of polypropylene/montmorillonite nanocomposites. *J. Polym. Sci. Polym. Phys.* **2002**, *40*, 408–414.

40. Sharma, S.K.; Nayak, S.K. Surface modified clay/polypropylene (PP) nanocomposites: Effect on physico-mechanical, thermal and morphological properties. *Polym. Degrad. Stab.* **2009**, *94*, 132–138.

41. Sharma, S.K.; Nema, A.K.; Nayak, S.K. Polypropylene nanocomposite film: A critical evaluation on the effect of nanoclay on the mechanical, thermal, and morphological behavior. *J. Appl. Polym. Sci.* **2010**, *115*, 3463–3473.

42. Naffakh, M.; Díez-Pascual, A.M.; Marco, C.; Ellis, G. Novel polypropylene/inorganic fullerene-like WS$_2$ nanocomposites containing a β-nucleating agent: Mechanical, tribological and rheological properties. *Mater. Chem. Phys.* **2014**, *144*, 98–106.

43. Gao, F.G.; Beyer, G.; Yuan, Q.C. Mechanistic study of fire retardancy of carbon nanotube/ethylene vinyl acetate copolymers and their clay composites. *Polym. Deg. Stab.* **2005**, *89*, 559–564.

44. Haiyun, M.; Lifang, T.; Zhongbin, X.; Zhengping, F. Synergistic effect of carbon nanotube and clay for improving the flame retardancy of ABS resin. *Nanotechnology* **2007**, *18*, 375602–375610.

45. Cui, Y.H.; Wang, X.X.; Li, Z.Q.; Tao, J. Fabrication and properties of Nano-ZnO/Glass fiber reinforced polypropylene composites. *J. Vinyl. Addit. Technol.* **2010**, *16*, 189–194.

46. Jacob, S.; Suma, K.K.; Mendaz, J.M.; George, A.; George, K.E. Modification of polypropylene/glass fiber composites with nanosilica. *Macromol. Symp.* **2009**, *277*, 138–143.

47. Díez-Pascual, A.M.; Naffakh, M.; Gómez-Fatou, M.A. Mechanical and electrical properties of novel poly(ether ether ketone)/carbon nanotube/inorganic fullerene-like WS_2 hybrid nanocomposites: experimental measurements and theoretical predictions. *Mater. Chem. Phys.* **2011**, *130*, 126–133.

48. Naffakh, M.; Díez-Pascual, A.M.; Marco, C.; Ellis, G. Morphology and thermal properties of novel poly(phenylene sulfide) hybrid nanocomposites based on single-walled carbon nanotubes and inorganic fullerene-like WS_2 nanoparticles. *J. Mater. Chem.* **2012**, *22*, 1418–1425.

49. Díez-Pascual, A.M.; Naffakh, M. Mechanical and thermal behaviour of isotatic polypropylene reinforced with inorganic fullerene-like IF-WS_2 nanoparticles: Effect of filler loading and temperature. *Mater. Chem. Phys.* **2013**, *141*, 979–989.

50. Ashrafi, B.; Diez-Pasual, A.M.; Johnson, L.; Genest, M.; Hind, S.; Martínez-Rubi, M.; González-Domínguez, J.M.; Martínez, M.T.; Simard, B.; Gómez, M.A.; *et al.* Influence of interfacial characteristics on properties of PEEK/Glass fiber laminates modified with single-walled carbon nanotubes. *Compos. Part A* **2012**, *43*, 1267–1279.

51. Díez-Pascual, A.M.; Naffakh, M.; Gómez, M.A.; Marco, C.; Ellis, G.; Martinez, M.T.; Anson, A.; Gónzaelz-Dominguez, J.M.; Martinez-Rubi, Y.; Simard, B. The influence of a compatibilizer on the thermal and dynamic mechanical properties of PEEK/carbon nanotube composites. *Nanotechnology* **2009**, *20*, doi:10.1088/0957-4484/20/31/315707.

52. Díez-Pascual, A.M.; Ashrafi, B.; Naffakh, M.; González-Domínguez, J.M.; Johnston, A.; Simard, B.; Martínez, M.T.; Gómez, M.A. Influence of carbon nanotubes on the thermal, electrical and mechanical properties of PEEK/glass fiber laminates. *Carbon* **2011**, *49*, 2817–2833.

53. Díez-Pascual, A.M.; Naffakh, M.; Marco, C.; Gómez, M.A.; Ellis, G. Multiscale fiber-reinforced thermoplastic composites incorporating carbon nanotubes: A review. *Curr. Opin. Mater. Sci.*, in press.

54. Rahmanian, S.; Thean, K.S.; Suraya, A.R.; Shazed, M.A.; Salleh, M.A.M.; Yusoff, H.M. Carbon and glass hierarchical fibers: Influence of carbon nanotubes on tensile, flexural and impact properties of short fiber reinforced composites. *Mater. Des.* **2013**, *43*, 10–16.

55. Joshi, H.; Purnima, J. Development of glass fiber, wollastonite reinforced polypropylene hybrid composite: Mechanical properties and morphology. *Mater. Sci. Eng. A* **2010**, *527*,1946–1951

56. Haribabu, J.; Sir, K.A.; Ravikiran, B. Fabrication and characterization of PPS/40%GF/nano-$CaCO_3$ hybrid composites. *Int. J. Mod. Eng. Res.* **2013**, *3*, 2262–2266.

57. Narayana, S.; Suman, K.N.S.; Babu, S.R.; Ramesh, N. Effect of nano-$CaCO_3$ content on flexural and impact properties of PPS/GF ternary composites. *Int. J. Eng. Res. Technol.* **2012**, *1*, 1–7.

58. Lopez-Gaxiola, D.L.; Jubinski, M.M.; Keith, J.M.; King, J.A.; Miskioglu, I. Effects of carbon fillers on tensile and flexural properties in polypropylene-based resins. *J. Appl. Polym. Sci.* **2010**, *118*, 1620–1633.

59. Díez-Pascual, A.M.; Naffakh, M.; Marco, C.; Ellis, G. Rheological and tribological properties of carbon nanotube/thermoplastic nanocomposites incorporating inorganic fullerene-like WS$_2$ nanoparticles. *J. Phys. Chem. B* **2012**, *116*, 7959–7969.

60. Díez-Pascual, A.M.; Naffakh, M.; Marco, C.; Ellis, G. Mechanical and electrical properties of carbon nanotube/polyphenylene sulphide composites incorporating polyetherimide and inorganic fullerene-like WS$_2$ nanoparticles. *Compos. Part A* **2012**, *43*, 603–612.

61. Rapoport, L.; Nepomnyashcy, O.; Verdyan, A.; Popovitz-Biro, R.; Volovik, Y.; Ittah, B.; Tenne, R. Polymer nanocomposites with fullerene-like solid lubricant. *Adv. Eng. Mater.* **2004**, *6*, 44–48.

62. Friedrich, K.; Schlarb, A.K. *Tribology of Polymeric Nanocomposites*; Briscoe, B.J., Ed.; Elsevier: Amsterdam, The Netherlands, 2008.

63. Wang, Q.H.; Xu, J.; Shen, W.; Xue, Q. The effect of particle size of nanometer ZrO2 on the tribological behaviour of PEEK. *Wear* **1997**, *209*, 316–321.

64. Shwartz, C.J.; Bahadur, S. Studies on the tribological behavior and transfer film-counterface bond strength for polyphenylene sulfide filled with nanoscale alumina particles. *Wear* **2000**, *237*, 261–273.

65. Kanny, K.; Jawahar, P.; Moodley, V.K. Mechanical and tribological behavior of clay polypropylene nanocomposites. *J. Mater. Sci.* **2008**, *43*, 7230–7238.